Mechanical Properties and Swelling Behavior of End-Linked Poly(diethylsiloxane) Networks

Ronald C. Hedden, Himanshu Saxena, and Claude Cohen*

School of Chemical Engineering, Olin Hall, Cornell University, Ithaca, New York 14853

Received August 14, 2000; Revised Manuscript Received September 15, 2000

ABSTRACT: Linear α,ω-vinyl-terminated poly(diethylsiloxane) (PDES) chains were synthesized and fractionated to obtain melts of low polydispersity. The fractionated samples were characterized using gel permeation chromatography and dilute solution viscometry. PDES elastomers were also prepared from the melts using hydrosilylation end-linking. The effects of chain stiffness on solution viscometric properties and on network swelling in toluene were compared to previously obtained results with poly(dimethylsiloxane) (PDMS). The mechanical behavior of the PDES elastomers in uniaxial extension was studied with a Perkin-Elmer dynamic mechanical analyzer. The dry networks exhibit a stress-induced amorphous-to-mesophase transition, which results in a discontinuous stress−strain relationship. The effects of molecular-level structure on network mechanical properties were deduced by studying PDES elastomers with well-defined molecular weight between chemical cross-links.

Introduction

Poly(diethylsiloxane), PDES, is a semiflexible homopolymer that exhibits complex and unusual phase behavior. The phase behavior of (non-cross-linked) PDES has been thoroughly documented.[1−14] At temperatures below about 280 K, PDES chains can exist in two distinct crystalline phases. The structures of these phases have been identified as a kinetically formed pseudo-monoclinic α phase and a thermodynamically stable pseudo-tetragonal β phase.[6] The relative proportions of the α and β crystal phases in a given sample depend on its thermal history. The crystalline phases may be further classified as low-temperature polymorphs α1 and β1 or high-temperature polymorphs α2 and β2. Upon heating, the α1 and β1 phases undergo first-order crystal−crystal transitions to α2 and β2 phases (α1 → α2 at 214 K; β1 → β2 at 206 K). This crystal−crystal transition has been attributed to the onset of trans−gauche conformational transitions within the polymer backbone.[14] Some authors have also reported observing additional crystalline phases (named γ1 and γ2), which may be structurally similar to the β phases.[13] At higher temperatures, the crystalline phases melt into a conformationally disordered mesophase μ, in which the ethyl side groups were found to have complete freedom of rotation around the polymer backbone (α2 → μ at 280 K; β2 → μ at 290 K).[14] The mesophase can only be observed in samples with molecular weight above about 28 000 g/mol.[11] At still higher temperature (depending on the sample molecular weight), the mesophase becomes an isotropic melt. Samples with low molecular mass will bypass the mesophase entirely, passing from the crystalline phases directly into the amorphous melt.

Cross-linked networks of PDES are capable of forming similar α, β, γ, μ, and amorphous phases.[13] A striking phenomenon exhibited by amorphous PDES networks is their ability to undergo a stress-induced transition to the mesophase. An initially amorphous PDES network placed under uniaxial tension can form a "neck" region consisting of an aligned birefringent mesophase region.[15,16] The structure of this neck region (as determined by X-ray diffraction measurements)[16] is similar to that of the μ phase observed in the melt. The formation of the mesophase can result in discontinuous stress−strain relationships under appropriate conditions of temperature and molecular weight between cross-links.

The properties of PDES networks are of interest since these materials could be applied in such devices as stress−optical switches or membranes for separation processes. From a fundamental science standpoint, the ethyl substituents restrict the motion and configuration of the polymer backbone as compared to PDMS affecting the stiffness and the packing of the chains.

Previous studies on PDES elastomers documented their phase behavior and swelling[13] and their mechanical properties.[15,16] It was observed that amorphous PDES networks exhibit unique mechanical properties such as strongly nonlinear relationships between stress and strain. Furthermore, a phase transition can be induced in these networks by applying stress or by decreasing temperature. Such behavior is typically exhibited by the more chemically complex cross-linked nematic liquid-crystalline polymer networks.[17−21] The mechanical properties of PDES elastomers have not been investigated in terms of their molecular-level structure because the previous studies have involved rather ill-defined architectures. Some studies involved PDES networks synthesized by random cross-linking of precursor chains by peroxide vulcanization,[7,15,22] which results in a wide distribution of elastic chain sizes between cross-links. Others[13] have synthesized PDES networks by hydrosilylation end-linking, but their networks had very high soluble fractions and thereby numerous imperfections. In this work, we establish connections between network structure and mechanical properties by preparing and studying a series of elastomers with well-defined structures. The soluble fraction was previously shown to be a very good indicator of the degree of perfection of a network.[23,24] We have prepared a series of end-linked PDES elastomers by minimizing the resulting soluble fraction at the end of cure. These networks have a minimum of structural defects and are thus named optimal end-linked elastomers. Imperfect networks with greater amounts of structural defects have also been prepared for comparison. The structure of the networks was systematically varied by using

10.1021/ma001419c CCC: $19.00
Published on Web 10/25/2000

precursor chains of different molecular weights. We have characterized the mechanical and swelling properties of these networks to provide the desired links between structure and physical properties.

Experimental Procedures

Monomer Synthesis. The monomer hexaethylcyclotrisiloxane (D_3Et_6) was prepared by a reaction previously described,[25] with some modifications. The reaction was carried out in a 1000 mL, three-neck round-bottom flask equipped with a condenser, a thermometer, and a dropping funnel. 76.8 g of zinc oxide powder (99.9%, Aldrich) and 300 mL of methyl acetate (99%, Aldrich) were added to the flask, and a suspension of the ZnO was formed by rapid stirring. 100 g of diethyldichlorosilane (Gelest, Inc.) dissolved in 150 mL of methyl acetate was then added via the dropping funnel over a period of about 1 h. The reaction was allowed to proceed for an additional 1.5 h with rapid stirring, during which time the mixture cooled to room temperature (23 °C). The reaction mixture was neutralized by addition of 800 mL of saturated aqueous sodium bicarbonate (Mallinckrodt) and was stirred for 1 h. The resulting two-phase mixture was vacuum filtered through Whatman brand filter paper, and the organic layer was retained. The aqueous layer was extracted twice with 140 mL of diethyl ether (Fisher), and the resulting ether layers were combined with the original organic layer. The diethyl ether and methyl acetate were removed by distillation in a Rotavapor apparatus. We prefer methyl acetate (rather than ethyl acetate) as a solvent due to its lower boiling point, which permits easier solvent removal. The product mixture was dried overnight using sodium sulfate (Fisher) and then filtered to remove the sodium sulfate. The product was then dried for 1 day over freshly powdered calcium hydride (Alfa Aesar, 88−96%). The product mixture was then vacuum-distilled over the calcium hydride, yielding 24 g (37%) of D_3Et_6 on average. The product was determined to be nearly 100% pure by gas chromatography.

Polymerization. α,ω-Vinyl functionalized PDES was produced from the D_3Et_6 monomer by cationic polymerization with trifluoromethanesulfonic acid as an initiator by the method first reported in ref 13. We chose the concentrations of the reactants to provide a high percentage of chains with vinyl end groups.

The monomer was vacuum distilled over calcium hydride (in some cases twice) immediately before reaction. Divinyltetramethyldisiloxane (97%, Aldrich) was purified by the same method before use. The reaction was carried out in a flame-dried, nitrogen-purged 50 mL round-bottom flask equipped with a rubber septum and magnetic stir bar. 20 g of D_3Et_6 monomer and 376 μL of divinyltetramethyldisiloxane were transferred into the flask by standard cannulation techniques. 7.2 μL of trifluoromethanesulfonic acid (99%+, Aldrich) was added by syringe to start the reaction. The polymerization was terminated after 5 days by addition of 1 mL of triethylamine (Fisher). The product was washed repeatedly with warm (55 °C) ethanol to remove cyclic byproducts and oligomers.

Polymer yield was typically 70−80%, depending somewhat on the number of ethanol washings. The number-average molecular weight of the product was about 10 000 g/mol (gel permeation chromatography), and M_w/M_n ratios of about 1.8−1.9 were obtained. Using a high concentration of divinyltetramethyldisiloxane permitted excellent vinyl end-functionalization of the chains but yielded chains of low molecular mass. Five batches of PDES produced by this technique were used in this study. They were labeled PDES-T1, PDES-T2, etc. PDES-T2 and PDES-T5 were prepared from perdeuterated D_3Et_6 monomer (5% CD_2CH_3 and 25% CD_2CH_3, respectively) for subsequent study by ^2H NMR spectroscopy.

To expand the range of molecular weights studied, a few batches of PDES were prepared with the NaOH/12-crown-4 catalyst/promoter system, using vinyldimethylchlorosilane (Gelest, Inc.) (in the presence of pyridine) as an end-capping reagent. The details of this procedure have been published elsewhere.[26] The oligomeric PDES samples labeled PDES-C1 and PDES-C2 had lesser degrees of vinyl functionalization than the PDES obtained from cationic polymerization, judging from the moduli and soluble fractions of the networks obtained. The batch PDES-C3 was a high molecular weight sample that was not used for making networks but was included in the intrinsic viscosity studies.

Fractionation. To obtain samples of low polydispersity, we fractionated the synthesized PDES melts using toluene as a good solvent and methanol as a poor solvent. This strategy also permitted us to get samples of higher molecular weight from the original batch. The starting concentration of PDES in toluene was 1.0 wt %. The fractions typically had M_w/M_n of about 1.1−1.3. The fractionation served to further remove small molecules and impurities, resulting in very clean samples ideal for end-linking reactions.

The PDES fractions were analyzed by gel permeation chromatography (GPC) to determine the number-average and weight-average molecular weights. The GPC consisted of a Waters model 6000A solvent delivery system, two Waters Styragel columns (models HR-3 and HR-4), and a Waters model R401 refractive index detector. All samples were run at 21 °C with toluene as the solvent at a flow rate of 1.0 cm^3/min. Calibration was conducted with polystyrene standards from Scientific Polymer Products, Inc. Polystyrene-equivalent molecular weights are reported throughout this study. Selected samples were checked on another GPC system running with THF at 30 °C, and nearly identical molecular weights were obtained.

Viscometry. Intrinsic viscosities of selected PDES fractions were measured in tetrahydrofuran at 30 °C with a Viscotek model 110 automatic viscometer. Further viscometry measurements were carried out in dilute toluene solutions at 25 °C with a Cannon Ubbelohde viscometer (capillary size 50) and an automatic timer. The Ubbelohde viscometer experiments were conducted with polymer concentrations no higher than 1.0 g/dL.

Network Preparation. Networks were prepared by hydrosilylation end-linking of the vinyl-end-capped precursors in the melt with the tetrafunctional cross-linker tetrakis(dimethylsiloxy)silane, or A_4 (Gelest, Inc.). The catalyst *cis*-dichlorobis(diethyl sulfide)platinum(II) (Strem Chemicals, Inc.) was prepared in toluene solution at a concentration of 0.0023 g of catalyst/1.0 mL of toluene. 20.0 μL of the catalyst solution was added per gram of polymer.

The mole ratio of Si−H groups:vinyl groups which yields optimum networks (those with the fewest structural defects and highest modulus) is not necessarily 1:1. An excess of Si−H groups is required, in part due to the presence of some side reactions that consume Si−H.[27] The mole ratio of Si−H to vinyl used was denoted r and is defined by

$$r = \frac{4(\text{moles of } A_4)}{2(\text{moles of ploymers})} \quad (1)$$

The optimum value, r_{opt}, for a given polymer sample was determined by trial and error. r_{opt} was taken as the ratio yielding a network with the highest modulus and lowest degree of equilibrium swelling.[24] r_{opt} for this polymer was between 1.2 and 1.6 for most of the samples studied, depending somewhat on the precursor molecular weight. In general, the larger the precursor molecular weight, the higher the value of r_{opt}.[23]

The networks were cast into rectangular, 1.25 mm thick films by curing in a glass mold. The mold was left open at the top, exposing the thin edge of the sample, so gaseous byproducts could escape during curing. To prevent gas bubbles from forming in the network, the reaction mixture was placed under vacuum for the first few minutes of curing. The volatility of the A_4 cross-linker is sufficiently low such that it did not evaporate significantly during the vacuum procedure. The films were then cured at 35 °C for 3 days under air. A postcure at 70 °C was conducted for 2−3 days to ensure complete reaction. The curing of the PDES networks was slower than in the case of PDMS networks.[24]

Samples for dynamic mechanical analysis were punched out of the film using a rectangular steel "cookie cutter" device. In this manner, samples with smooth surfaces and very regular dimensions could be obtained for mechanical analysis. Rectangular samples were preferred over the standard "dog bone" samples due to the relatively simple cutting of small rectangles from the molded elastomer sheets.

Swelling Experiments. The soluble fractions of the networks were extracted in toluene to remove impurities and unattached chains. The networks were swollen for at least 3 days, and the solvent was replaced with fresh toluene every day. Networks were deswollen by progressively adding methanol to the toluene over a period of several days. The networks were dried for 2 days or more under air. The soluble fraction was computed as the weight fraction of soluble material removed during swelling. The swelling ratio was computed from the relationship

$$Q = 1 + \frac{M_s - M_{ext}}{M_{ext}}\left(\frac{\rho_2}{\rho_1}\right) \qquad (2)$$

where Q is the swelling ratio, M_s is the swollen mass (of the network and solvent combined), M_{ext} is the dry weight of the network after extraction, and ρ_1 and ρ_2 are the densities of toluene (0.865 g/cm^3) and PDES (0.99 g/cm^3), respectively.

Dynamic Mechanical Analysis. A Perkin-Elmer DMA 7e was used for all mechanical measurements. The temperature could be held constant or increased linearly by use of the standard Perkin-Elmer "small" furnace. The furnace was also connected to a recirculating cooling bath that could bring the temperature down to −30 °C.

The elastic (Young's) moduli of the PDES networks were measured in uniaxial extension. The elastic moduli at 25 °C were measured at a strain of approximately 1% and were converted to equilibrium shear moduli, G_e, through the previously established[28] relationship $E = 3G_e$. The cross-sectional area of a sample was assumed not to change appreciably under the small strains studied. Two different sets of thermomechanical measurements were also performed on the samples:

(1) Strain−temperature scans: Samples were loaded with a constant uniaxial extension force. After the initial loading of the sample, the temperature was reduced to −10 °C to accelerate the formation of the mesophase. After the length of the sample stabilized (typically after 3−5 h), the sample consisted of two regions: (i) A semicrystalline or mesomorphic structure in a highly birefringent neck and (ii) a rubberlike, completely amorphous end regions that have a greater width (about a factor of 2) than the neck. A temperature ramp was then performed under constant applied force at a rate of 0.5 °C/min to a temperature of about 35 °C. The length of the sample was recorded as a function of temperature throughout the experiment.

(2) Strain−stress scans: Samples were allowed to equilibrate under a constant uniaxial extension force (5−6 h). An inverse stress ramp with stress rate of 972 Pa/min was started, and the length of the sample was monitored. At this rate of stress change, the sample had time to equilibrate with the imposed stress. This assumption was verified by imposing a stress rate ramp lower by a factor of 2 and obtaining nearly identical results.[29] We also studied the engineering stress−strain relationships for the samples at various temperatures.

Results and Discussion

Viscometry. Intrinsic viscosities [η] in THF at 30 °C and in toluene at 25 °C are listed in Table 1. Because of the low polydispersities of the samples, the weight-average molecular weight can be taken to approximate the viscosity-average molecular weight. The intrinsic viscosity results were analyzed using Stockmayer−Fixman plots[30] (Figure 1). The results in THF show deviation from linear behavior at high M_w (above 100 kg/mol). This deviation is expected[31] at high M_w, since only the linear term is kept in the expansion of $[\eta]/M_w^{0.5}$

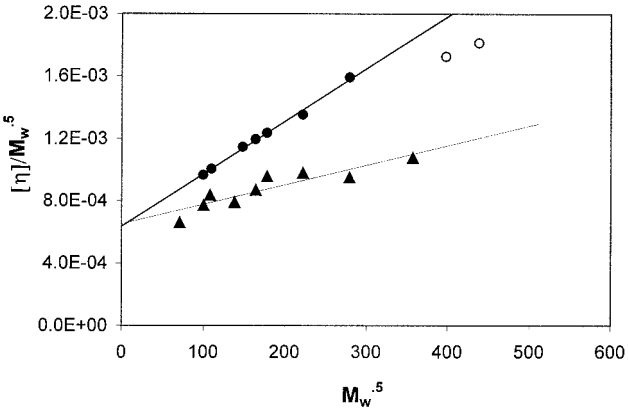

Figure 1. Stockmayer−Fixman plots of the intrinsic viscosity data of PDES in toluene (triangles) and in THF (circles).

Table 1. Viscometry Results

sample	M_w (kg/mol)	M_w/M_n	[η], dL/g THF, 30 °C	[η], dL/g toluene, 25 °C
PDES-C4	5.1	1.22		0.047
PDES-T2-d2 (V)	9.9	1.09	0.096	0.077
PDES-T1(V)	11.7	1.19		0.091
PDES-T2-d2 (IV)	12.0	1.12	0.110	
PDES-T1 (IV)	19.0	1.18		0.109
PDES-T4 (V)	22.0	1.09	0.170	
PDES-T4 (IV)	26.8	1.11	0.196	0.143
PDES-T4 (III)	31.6	1.13	0.220	0.171
PDES-T4 (I)	49.2	1.19	0.300	0.218
PDES-C3 (IV)	77.9	1.19	0.444	0.266
PDES-C3 (III)	127.3	1.31		0.384
PDES-C3 (II)	157.9	1.25	0.686	
PDES-C3 (I)	191.6	1.43	0.794	

in $M_w^{0.5}$ in the Stockmayer−Fixman analysis. For THF, only the data points below M_w = 85 kg/mol were used for further analysis. In toluene, data were collected up to M_w = 127 kg/mol, and no deviations from the expected behavior could be observed within the limits of experimental uncertainty. The precision of the viscosity data in THF (automated Viscotek viscometer) was noticeably better than that of the data in toluene (Ubbelohde viscometer).

The limiting slopes of the Stockmayer−Fixman plots were used to determine a polymer−solvent interaction parameter χ_0 at very dilute polymer concentration. χ_0 was determined from the relationship

$$\text{slope} = 0.51\Phi_0\left(\frac{v_2^2}{v_1 N_A}\right)(1 - 2\chi_0) \qquad (3)$$

where Φ_0 is a "universal" viscosity constant[32,33] taken to be 2.5 × 10^{23} mol^{-1}; v_2 is the specific volume of the polymer, which is taken to be 1.01 cm^3/g; v_1 is the molar volume of the solvent (106.5 cm^3/mol for toluene, 81.1 cm^3/mol for THF); and N_A is Avogadro's number. Using eq 3, χ_0 is 0.467 for PDES in toluene, which is slightly above the measured value of 0.458 for PDMS in toluene.[34] χ_0 is 0.412 for PDES in THF at 30 °C, indicating that THF is a better solvent than toluene for PDES near room temperature. The observation that the intrinsic viscosities in THF were substantially higher than those in toluene indicates that the PDES chains occupy a larger hydrodynamic volume in THF solution, assuming the effect of the temperature difference to be negligible.

The intercept of the Stockmayer−Fixman plot yields the parameter K_θ, which has a measured value of 6.5×10^{-4} (dL/g)(g/mol)$^{-0.5}$ in toluene and 6.4×10^{-4} (dL/g)(g/mol)$^{-0.5}$ in THF. These values are in good agreement, although the value of K_θ in toluene has a fairly high uncertainty. For comparison, a value of $K_\theta = 7.94 \times 10^{-4}$ (dL/g)(g/mol)$^{-0.5}$ has been previously reported for PDMS in toluene.[34]

The plateau modulus and entanglement molecular weight of PDES can be estimated from K_θ by the method of Fetters et al.[35,36] The estimated plateau modulus can be found at 298 K from the semiempirical relation

$$G_N^0 = [3.68 \times 10^5 \text{ MPa cm}^9 \text{ mol}^{-1} \text{ dL}^{-2}] K_\theta^2 \rho^3 \quad (4)$$

where ρ is the density of the polymer in the melt at 298 K, taken to be 0.99 g/cm^3. Using the viscometry data in THF, the value of G_N^0 obtained for PDES is 1.45×10^5 Pa, whereas G_N^0 of PDMS is calculated to be 2.15×10^5 Pa. The molecular weight between entanglements is obtained from the relationship[35,36]

$$M_e = \rho RT/G_N^0 \quad (5)$$

By eq 5, M_e of PDES is estimated to be 17 200 g/mol, as opposed to 11 500 g/mol for PDMS. The calculated values for M_e and G_N^0 indicate that PDES chains are stiffer than PDMS, consistent with previously reported values for the Kuhn lengths—1.96 nm for PDES and 1.56 nm for PDMS.[39] The larger side groups in PDES compared to PDMS have a significant effect on the chain stiffness and the molecular weight between entanglements. Values for G_N^0 and M_e may also be obtained from small-angle neutron scattering measurements of the chain dimensions in the melt, a method which is believed to be a more reliable method than viscometric analysis.[35] SANS measurements of labeled PDES are planned by the authors in the near future.

The empirical correlations obtained by Fetters et al. also allow for the calculation of two parameters that ensue from the concept of entanglement formation in a polymer; these are the tube diameter d_t and the packing length p.[35,36]

$$d_t = [0.537 \text{ Å dL}^{2/3} \text{ cm}^{-3} \text{ mol}^{1/3}] K_\theta^{-2/3} \rho^{-1} \quad (6)$$

and

$$d_t = 17.68p \quad (7)$$

At 298 K, one obtains $d_t \approx 64$ Å and $p \approx 3.63$ Å from the values of K_θ and ρ for PDMS,[34] whereas for PDES, these values are estimated to be 73 and 4.15 Å, respectively. It is not surprising that PDES would have a larger reptation tube diameter than PDMS, given its larger side groups. The ratio of the Kuhn lengths[39] for PDES:PDMS is 1.26, whereas the ratio of the packing lengths is found to be 1.14.

Viscometry results were also used to find the parameters K and a of the Mark−Houwink relation between M_w and the intrinsic viscosity:

$$[\eta] = KM_v^a \quad (8)$$

Since the polydispersities of the samples were low, M_w was again taken to be a good estimate of M_v. The best fits to the data are

$$[\eta] \text{ (g/dL)} = 1.37 \times 10^{-4} M_w^{0.715} \quad \text{(THF, 30 °C)} \quad (9a)$$

$$[\eta] \text{ (g/dL)} = 1.15 \times 10^{-4} M_w^{0.704} \quad \text{(toluene, 25 °C)} \quad (9b)$$

The values of the exponent a, together with the calculated χ_0 parameters, indicate that THF is a slightly better solvent than toluene for PDES, assuming negligible effect due to temperature difference.

Equilibrium Swelling and Modulus Measurements. The characteristics of the networks prepared are listed in Table 2. Soluble fractions, equilibrium swelling results in toluene, and moduli of the dry samples measured at 25 °C are reported. We estimate the molecular weight between effective cross-links for each sample by the relationship[37]

$$M_c = \frac{\rho RT}{G_e} \quad (10)$$

The soluble fractions of the networks are an indicator of the degree of perfection of the end-linked structure. The networks listed as optimal networks had an Si−H:vinyl ratio at or near the optimum value of "*r*" ($r_{opt} \approx 1.5$ over the molecular weight range studied) and have, with one exception, a soluble weight fraction of about 1%. Data on other networks are also reported. The linear precursors for our optimal networks (fractions of batches PDES-T1 and PDES-T5) must have had a very high degree of vinyl end-functionalization to result in such low soluble fractions. The batches PDES-T2-d2, PDES-T3, and PDES-C1 had lesser degrees of vinyl functionalization, resulting in networks with higher soluble fractions. The degree of vinyl functionalization of the chains prepared by cationic polymerization was found to be best when the monomer was purified repeatedly before polymerization (PDES-T1 and PDES-T5). For the PDES chains prepared with the NaOH/12-crown-4 catalyst, only low molecular weight chains such as PDES-C1 could be satisfactorily end-capped with vinyl. We are not sure why vinyl end groups could not be added to the high molecular weight samples synthesized by this method.

The optimal networks in Table 2 are the only reported PDES networks to date with controlled molecular architecture. Previous studies on PDES networks generally involved random cross-linking[15,16] or incompletely functionalized precursor chains,[13] resulting in materials with somewhat ill-defined structures. Our optimal end-linked networks enable us to demonstrate the connection between precursor molecular weight and network mechanical properties.

Figure 2 shows the moduli of the optimum networks as a function of precursor molecular weight. The networks with the smallest precursor chains have the highest cross-link density and the highest modulus. As the molecular weight of the chains is increased, the moduli of the dry networks approach a limiting value of about $G = 1.8 \times 10^5$ Pa. This number is slightly above the calculated plateau modulus, $G_N^0 = 1.45 \times 10^5$ Pa. In the high precursor molecular weight limit, the number of trapped entanglements in the network exceeds the number of chemical cross-links. The effective cross-link density is dominated by the entanglements. Thus, the network shear modulus approaches G_N^0, the plateau modulus of a highly entangled melt. This trend has also been noted in the case of model

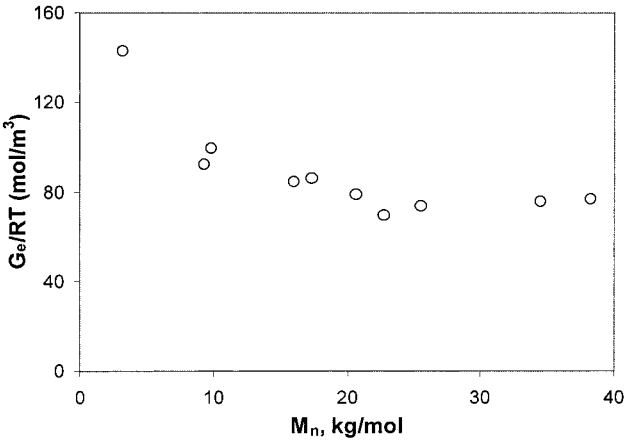

Figure 2. Reduced elastic shear modulus of optimal end-linked PDES networks as a function of precursor molecular weight.

Table 2. PDES Network Characteristics

sample	precursor M_n	M_w (kg/mol)	G_e/RT (mol/m^3)	M_c (kg/mol)	Q in toluene	W_{sol} (wt %)
			Optimal Networks			
H-1	34.5	48.7	75.5	13.1	3.93	0.3
H-2	25.7	32.8	73.6	13.5	3.90	1.1
H-3	22.9	28.1	69.2	14.3	4.02	1.2
H-5	20.8	25.4	78.5	12.6	3.76	1.0
H-8	9.8	11.7	99.3	9.97	3.33	1.4
H-12	3.2	3.7	143.0	6.92	2.56	3.6
A	38.3	50.5	76.8	12.9	3.71	0.4
C	25.6	31.2	79.1	12.5	3.65	N/M
D	19.9	24	77.4	12.8	3.69	N/M
E	17.4	20.4	85.8	11.5	3.49	0.5
G	9.3	11.1	92.1	10.7	3.36	1.0
			Other Networks			
H-4	20.8	25.4	71.9	13.8	3.81	N/M
H-6	16.0	19.0	84.2	11.8	3.49	N/M
H-7	16.0	19.0	82.8	11.9	3.53	N/M
H-9	9.8	11.7	95.7	10.3	3.17	1.5
H-10	9.8	17.6	40.3	24.6	5.11	9.5
H-11	9.8	17.6	44.7	22.2	4.86	8.1
H-13	10.6	15.5	48.1	20.6	4.90	9.4
Imp-1	18.3	24.5	56.0	17.7	4.45	3.6
Imp-2	18.3	24.5	52.3	18.9	4.56	3.9
Imp-3	14.5	18.0	51.0	19.4	4.53	4.6
Imp-4	14.5	18.0	44.7	22.1	4.95	N/M
Imp-5	11.8	14.0	42.9	23.1	5.06	6.5
Imp-6	11.8	14.0	41.0	24.2	5.19	6.9

[a] N/M = not measured.

Table 3. Swelling Comparison of PDES and PDMS Networks in Toluene at 25 °C

sample	G_e/RT (mol/m^3)	ϕ_2(toluene)
	PDES Networks	
Imp-4	44.7	0.202
H-11	44.7	0.206
H-4	71.9	0.262
H-2	73.6	0.256
H-6	84.2	0.287
H-12	143.0	0.390
	PDMS Networks (Data from ref 40)	
R1	45.8.	0.158
S1	72.2	0.219
N1	86.6	0.242
P2	140.9	0.306

PDMS networks.[24] Turning to the equilibrium swelling data in toluene, an interesting comparison to PDMS networks can be drawn. Table 3 shows swelling data in toluene for a few selected PDES and PDMS networks with comparable moduli. The data on PDMS networks

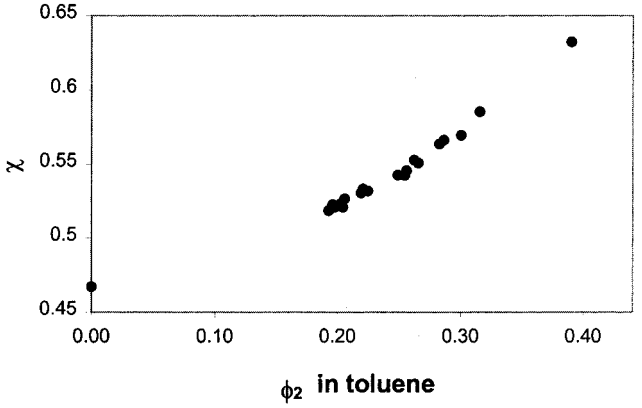

Figure 3. Interaction parameter as a function of polymer volume fraction obtained from the elastic modulus of the networks and the Flory−Rehner model. The datum on the *y*-axis is the value obtained from intrinsic viscosity measurements.

are from ref 40. Over the modulus range studied, the PDES networks swell appreciably less than their PDMS counterparts, despite the similar χ_0 parameters found from viscometric analysis.

One way to analyze the difference in swelling behavior is to look at the concentration dependence of the interaction parameter calculated from a model such as the Flory−Rehner model. The two versions of this model are[41,42]

$$\ln(1-\phi_2)+\phi_2+\chi\phi_2^{\,2}=v_1\left(\frac{G_e}{RT}\right)\left[\frac{\phi_2}{2}-\phi_2^{\,1/3}\right] \quad (11)$$

for what has been called the affine model of swelling, and

$$\ln(1-\phi_2)+\phi_2+\chi\phi_2^{\,2}=-v_1\left(\frac{G_e}{RT}\right)\phi_2^{\,1/3} \quad (12)$$

for the phantom model of swelling. In the above equations, v_1 is the molar volume of the solvent, taken to be 106.5 cm^3/mol for toluene. The affine model was applied to the data to extract the values of χ shown in Figure 3. The datum at $\phi_2 \approx 0$, χ_0, is the value calculated from viscometric measurements in dilute solutions. From the values of the χ_0 parameters of PDMS and PDES in toluene and the Mark−Houwink exponents, one might conclude that toluene is a solvent of similar quality for PDMS and PDES. The data of Table 3 comparing swelling results from PDMS and PDES networks of similar elastic modulus indicate, however, that at high polymer concentration toluene is comparatively a much better solvent for PDMS than for PDES.

The analysis of the swelling data by the Flory−Rehner model also leads to an interesting point about the determination of interaction parameters from network swelling. In the case of PDMS, a previous study[24] demonstrated that extrapolation of the network swelling data to zero concentration yields a χ_0 parameter which agrees with viscometry measurements of dilute solutions of PDMS chains.[24,34] The interaction parameter for PDES/toluene determined from viscometry also seems to be reasonable when plotted at $\phi_2 = 0$ as in Figure 3. However, the calculated χ parameters from the Flory−Rehner model are not always consistent with independent measurements from solutions. Our earlier work on networks of a 15% diphenyl/85% dimethylsiloxane random copolymer[43] swollen in toluene exempli-

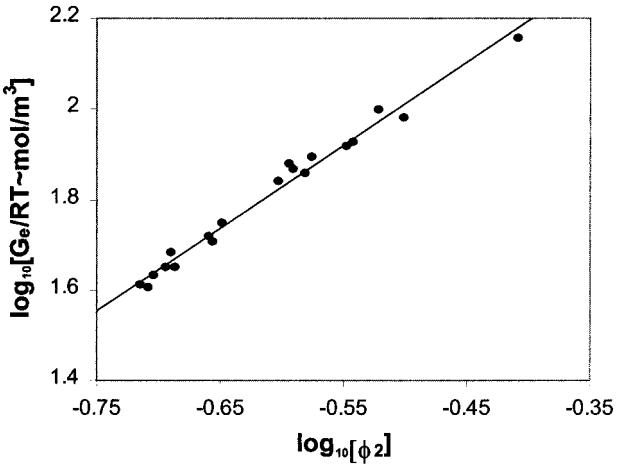

Figure 4. Relationship between the elastic modulus of PDES networks and their equilibrium swelling in toluene.

fies this situation. Other authors have noted similar discrepancies between χ(network) and χ(solution) for such systems as poly(vinyl alcohol)/water[44] and natural rubber/various solvents.[45] Discrepancies between measured network and solution thermodynamic properties in the poly(vinyl acetate)/(toluene or acetone) systems have been previously attributed to the observation that the mixing free energy in a network is not necessarily the same as that of a corresponding solution.[46] In the case of PDMS[24] and PDES (Figure 3) swollen in toluene, the apparent consistency between the value of χ_0 from dilute solution measurements and the values of χ obtained from the Flory−Rehner model may thus be fortuitous.

From the equilibrium swelling ratios Q in toluene (25 °C), we also determined a power law relation between modulus and equilibrium swelling for PDES networks. Figure 4 shows log(G_e/RT) versus log ϕ_2 for the networks in toluene (both optimal and imperfect networks). Here, ϕ_2 denotes the polymer volume fraction at equilibrium swelling and is equal to Q^{-1}. As in the case of PDMS networks,[24] the swelling data are seen to occupy a single curve, irrespective of the degree of perfection of the network structure. The swelling can be predicted on the basis of the modulus alone, regardless of relative amounts of elastic and pendent chains present. The power law between ϕ_2 and G_e/RT in the PDES/toluene system was determined to be

$$G_e/RT \sim \phi_2^{1.83} \tag{13}$$

within the range of values of the modulus of the networks studied. The exponent in eq 13 indicates a behavior close to that predicted by the theory of Obukhov et al.[46] for the swelling of networks in good solvents. Higher values of this exponent (1.91−2.3) have been reported for the PDMS/toluene system[40,47] and indicate the poorer quality of toluene vis-à-vis PDMS at high polymer concentration.

Strain−Temperature Measurements. Strain−temperature scans described in the Experimental Section were performed on three optimal networks: H-1, H-3, and H-5 (Table 2). Figure 5 shows the results for sample H-1. Similar results were obtained for the other two samples.[29] It was not possible to obtain strain−temperature scans for samples with lower values of M_c. Our lower-M_c (higher modulus) samples (such as H-8) were quite brittle, and it was difficult or impossible to obtain a stable biphasic (neck) region without breaking the sample.

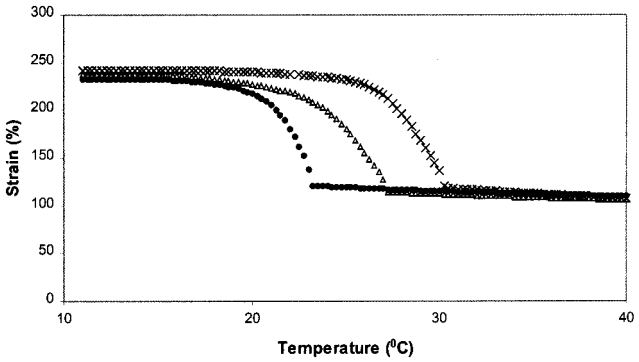

Figure 5. Strain−temperature curves for sample H-1 at three different values of the uniaxial force. Symbol notations: ● (2.1 × 10^5 Pa), △ (2.2 × 10^5 Pa), and × (2.3 × 10^5 Pa) where stress values are based on original cross section of the unstretched amorphous sample. The strain is measured under a fixed force while increasing the temperature at 0.5 °C/min.

Looking at Figure 5, as the temperature is increased at a constant uniaxial load, the length remains constant or decreases slowly at first. Then, at some temperature corresponding to the sudden "melting" of the neck region into an amorphous elastomer, the sample shrinks and the length decreases drastically. Higher loads on the sample cause higher transition temperatures. The minimum tensile force f_{eq} required to maintain equilibrium between the mesomorphic neck and the amorphous phases can be related to the transition temperature by the thermodynamic relation[48,49]

$$[\partial(f_{eq}/T)/\partial(1/T)]_p = \Delta H/\Delta L \tag{14}$$

where T may be regarded as the melting or transition temperature T_m.

By introducing the engineering stress σ_{eq} (referred to the amorphous isotropic cross section in the absence of any force) in eq 14 and by integrating it with the approximation that ΔS and ΔH are independent of temperature, one obtains

$$\sigma_{eq}/T_m = (\Delta H/V)L_i^a \int_{1/T_m{}^i}^{1/T_m} (\Delta L)^{-1}\, d(1/T) = (\Delta H/V)L_i^a J(1/T_m) \tag{15}$$

where $L_i{}^a$ is the length of the sample in the amorphous state in the absence of any force, $T_m{}^i$ is the equilibrium melting temperature for a tensile force f of zero, T_m is the equilibrium melting temperature for a tensile force f, V is the volume of the sample in the amorphous state, and $\Delta H/V$ represents the enthalpy changes upon melting of unit volume of mesomorphic structure (or semicrystalline phase) in the network. The function $J(1/T_m)$ defined by eq 15 may be evaluated by graphical integration. The latent enthalpy change associated with the transformation of the sample from the mesomorphic (or semicrystalline) structure to the amorphous state may then be computed in accordance with eq 15. Values of $L_i^a J(1/T_m)$ established by graphical integration of $(\Delta L)^{-1}$ plotted against $1/T$ for all three samples examined are shown in Figure 6 where σ_{eq}/T_m is plotted versus $L_i^a J(1/T_m)$. The slope of the straight line drawn through the three sets of points determines $\Delta H/V$ according to eq 15. Thus,

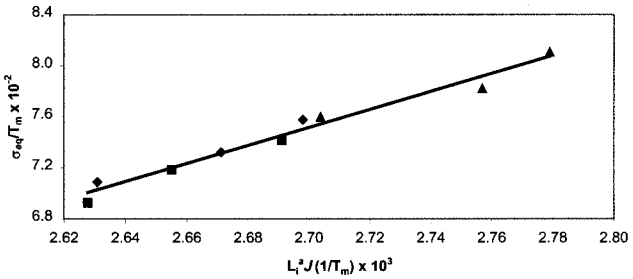

Figure 6. Plots of equilibrium stresses according to eq 15. Notations: ■ (H-3), ♦ (H-1), ▲ (H-5).

$$\Delta H/V = 7.06 \times 10^5 \text{ J/m}^3 = 0.706 \text{ J/cm}^3$$

where V is the volume of the sample in the amorphous state.

The quantity σ_{eq} denotes the engineering tensile stress required for equilibrium at T_m between the two structures. The latent change ΔH above represents the difference between the enthalpies of the two structures; that is, they refer to the process

partially crystalline (mesomorphic) network → amorphous network

We will assume here that the latent enthalpy change may be ascribed entirely to the melting of that mesophase fraction which is in the mesomorphic structure. Amorphous chains in both the amorphous phase and the mesomorphic structure are probably in a state of strain, but in the approximation that an amorphous network exhibits ideal rubber elasticity[41] (i.e., $(\partial H/\partial L)_{V,T} = 0$)), their associated enthalpy change is negligible. Hence, the latent enthalpy change for the hypothetical process

totally crystalline network → amorphous network

may be obtained merely by dividing $\Delta H/V$ given above by the fractional degree of crystallinity. Assuming that the fractional degree of crystallinity is x, and with further introduction of the specific volume, 1.01 cm^3/g for PDES, one obtains

$$\Delta H_{(\text{crystalline}\rightarrow\text{amorphous})} = 0.71/x \text{ J/g}$$

The fraction crystallinity in the biphasic (neck) region alone was obtained from solid-state ^{2}H NMR to be 35%.[50] The literature value of ΔH obtained for PDES melts from DSC measurements[22] (3 J/g) would suggest that the average crystallinity in our samples is on the order of 25%. This value is consistent with the NMR result because it is an average over both the biphasic (neck) region and the single-phase (amorphous) regions.

Because of the relatively high degree of chemical cross-linking in our samples, the fractional crystallinity is expected to be lower than previously reported results on PDES networks.[22] PDES networks of higher molecular weight precursors and lower degrees of cross-linking exist in the mesophase even in the absence of an external force. For these types of networks, Godovsky[22] estimated a fractional crystallinity of 90% for samples under uniaxial extension.

Although there is a clear analogy between the stress-induced mesophase formation in PDES and the stress-induced crystallization upon uniaxial stretching of crystallizable polymer networks, Godovsky and Valetskaya[51] pointed out an important difference between these processes. Thermodynamically, in a phase transition accompanied by a change in length, the relationship between force f and the temperature T is given by eq 14. When $\Delta H > 0$, normally $\Delta L < 0$, thus f/T will increase with T. This means that the temperature at the phase transition will increase with an increase in the applied tensile force at constant pressure. Equation 14 appears to hold during the isotropization of stretched mesophase networks as well as during the melting of stretched crystalline networks for which it was originally intended. However, the enthalpy of isotropization in mesophase networks is at least 1 order of magnitude smaller than that of melting of crystallites in crystalline networks.[51] Therefore, the force coefficient of the temperature of transition T, defined as dT/df, should be at least 1 order of magnitude higher for the isotropization of the mesophase elastomers in comparison with the melting of the stretched crystalline network. dT/df for natural rubber was estimated to be $0.5K/N$,[48] while for the PDES networks in this study, it is about $95K/N$. The difference arises from the large difference in ΔH: 80 J/g for natural rubber compared to only about 3 J/g for PDES.

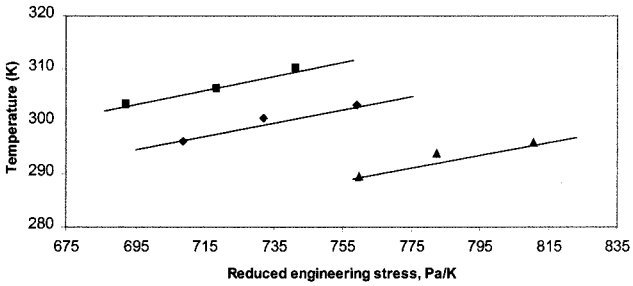

Figure 7. Variation of the transition temperature with reduced engineering stress (stress/temperature) for three networks. Solid lines are linear fits to the experimental values. Notations: ■ (H-3), ♦ (H-1), ▲ (H-5).

The transition temperature increases on increasing stress for each of the samples examined (see Figure 5). It is interesting to note from Figure 7 that the limited data obtained indicate that the transition temperature varies linearly with the reduced stress for the different samples examined. Such a linearity was originally predicted by de Gennes[52,53] for liquid crystalline elastomers on the basis of nematic interactions between mesogens. Many phenomenological descriptions that followed used the concept of nematic interactions to interpret the deviations of conventional elastomers away from the classical theories.[52−59] In particular, Warner et al.[57] used the concept of a semiflexible wormlike chain and nematic interactions between segments to again predict a linearity between reduced stress and transition temperature. These authors defined a reduced stress as $\sigma^* = \sigma/N_s k_B T$ where σ is the stress and N_s, k_B, and T are the number of elastic chains per unit volume, the Boltzmann constant, and the temperature, respectively. They predicted that the slope of the transition temperature versus σ^* curve should be inversely proportional to N_s, i.e., directly proportional to M_c. Although we qualitatively observe the predicted trend (Figure 7), it is not possible, unfortunately, to quantitatively establish this dependence based on the limited results we have obtained. We attempted to expand the data range by looking at samples with lower values of M_c, but these samples were too brittle to survive the DMA experiments.

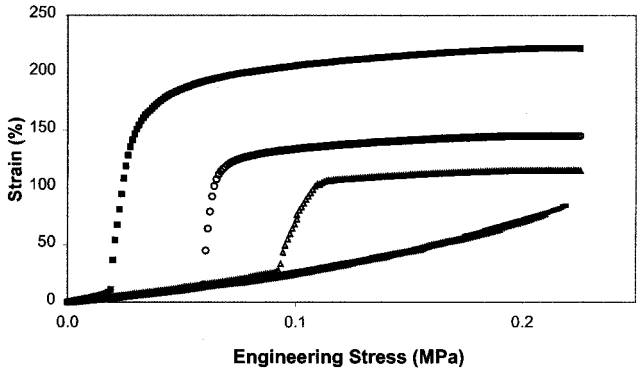

Figure 8. Engineering stress−strain curves for sample H-1 taken at different temperatures. Symbols: ■ (−7 °C), ○ (0 °C), △ (4.2 °C). Data at 7.5 and 20 °C are indistinguishable and do not show a transition. Stress was decreased from its maximum value at a rate of 944 Pa/min, and the corresponding strain was recorded.

Engineering Stress−Strain Measurements. Strain−stress scans described in the experimental procedures section were performed on the same three optimal networks considered above. Figure 8 shows the results for sample H-1. Similar results were obtained for the two other samples.[29] To check that the sample response to the applied stress is rapid compared to the stress rate of change and is not a delayed response, the strain measurements were repeated by changing the stress rate to half its value. The results from both stress rates were nearly identical, and the phase transformation took place at the same stress value.[29] This lends support to the premise that the experiments performed at 972 Pa/min show equilibrated strain values with the decreasing stress.

The nonlinearity in stress−strain relationship as evident from Figure 8 is very prominent at low temperatures. When stress is decreased at −7 °C on sample H-1 (Figure 8), the elastomer is mesomorphic up to a certain stress. Upon further decrease in stress, a very sharp drop in strain is observed, and the elastomer reaches an isotropic phase. On reducing the stress further, the elastomer response is similar to that of a conventional rubber, and an almost linear stress−strain behavior is seen. At higher temperatures, this mesomorphic−isotropic transition becomes less prominent, though it is still very sharp. At still higher temperatures (4.2 and 20 °C), the sample behaves as a conventional elastomer, and no transition is observed. Thus, each of these stress−strain curves consists of three portions. In the high stress region, the strain remains almost constant or decreases very slowly when stress is decreased. On decreasing the stress further, the sample shrinks very rapidly and the strain drops down, sometimes by as much as 80% of its initial value. The low stress portion of the curve is the region of relatively low degree of strain and follows a form similar to that of noncrystallizable amorphous elastomers.

The shape of the engineering stress−strain curve is determined by the relationship between the rate of stress change and the rate of mesophase formation or melting that depends on temperature. Figure 9 exhibits a hysteresis loop for sample H-1 at −7 °C. In the forward ramp, when the stress is increased at 972 Pa/min, the strain increases but remains much smaller than the corresponding values for the reverse ramp discussed above. This behavior is caused in part by the faster kinetics of melting of the mesophase as compared to the

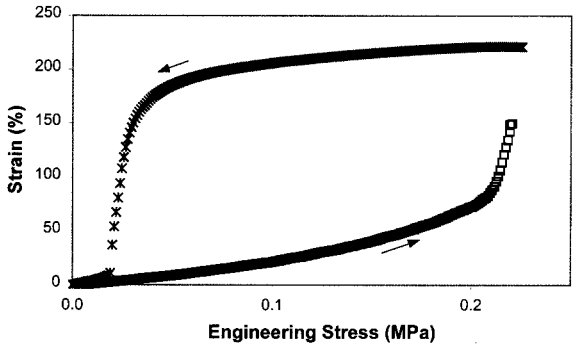

Figure 9. Strain hysteresis loop for sample H-1 at −7 °C. Both forward and reverse ramps are done at 972 Pa/min.

kinetics of formation of the mesophase and in part by the fact that the mesophase in the neck, in the ramp-down experiment, experiences a higher actual stress (by about a factor of 2) because of its smaller cross section. If one considers, for example, the state of the sample at the point where the engineering stress is 0.1 MPa in Figure 9, the sample is in the necked state during the decreasing stress ramp, whereas it is in the single phase (amorphous) state in the increasing stress ramp. In the forward ramp, it was observed that if the stress is held at some intermediate value, then the strain increases slowly until it reaches its equilibrium value. Thus, the shape of the stress−strain curve, as observed in Figure 9 on stretching (increasing stress ramp), is mainly kinetics limited. A stress−strain curve obtained during stretching (stress ramp-up) under reversible equilibrium will have, in principle, a similar shape as that obtained with a decreasing stress (ramp-down) if the entire sample is in the mesomorphic structure. Indeed, Godovsky et al.[16,17,50] have observed that the shape of the stress−strain curves during a forward stress ramp is the same as the curves obtained with the reverse stress ramp. The absence of hysteresis in their results is due to the fact that the PDES networks studied were synthesized from high molecular weight precursor chains and had high molecular weight between cross-links (M_c). Under these conditions, the samples were mesomorphic even in the absence of an external force.[15,51] The kinetics of mesophase formation in our amorphous samples synthesized from low molecular weight precursors is much slower due to a lack of nucleation sites that were abundant in the previously studied samples.[16,17,51] We note in Figure 9 that when the strain reaches a high value (∼80%), there is a delayed jump in the slope of the curve that is a manifestation of the formation of the mesophase.

The amorphous−mesomorphic transition caused by segment−segment interactions in a sample under uniaxial extension will also be influenced by the presence of a solvent.[58,59] We have performed isothermal stress ramp-down experiments on our PDES networks swollen with nonvolatile oligomeric poly(dimethylsiloxane) of molecular weight 2000 g/mol to determine the effect of a solvent on the mesophase formation under uniaxial force. Figures 10 and 11 show the engineering stress−strain behavior of network H-3 swollen in oligomeric PDMS. From Figure 10 it is observed that at $\phi = 0.9$ no mesophase was formed for temperatures higher than 0 °C, while for the dry network, the corresponding temperature was 18 °C.[29] Contrary to previously reported results on (hydroxypropyl)cellulose networks swollen in dimethyl sulfoxide,[19] Figure 11 shows that the force

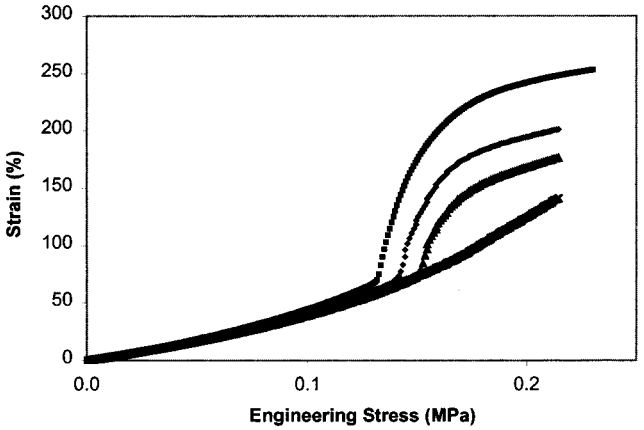

Figure 10. Engineering stress−strain curves for swelled sample H-3 ($\phi = 0.9$) taken at different temperatures. Notation: ■ (−7 °C), ♦ (−5.3 °C), ▲ (−3.4 °C), × (0.6 °C). Stress is decreased from its maximum value at a rate of 944 Pa/min, and the corresponding strain was recorded.

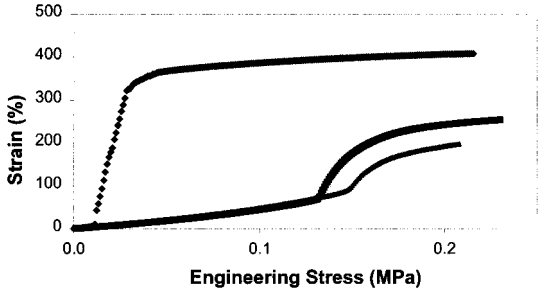

Figure 11. Engineering stress−strain curves for swelled sample H-3 at −7 °C for different swelling ratios: Notation: ♦ ($\phi = 1$), ■ ($\phi = 0.9$), ▲ ($\phi = 0.82$).

required for phase transformation is higher at lower volume fractions of the polymer, a result that is in agreement with theoretical predictions.[58,59] Also, the transformation from a mesomorphic structure to an amorphous phase appears less sharp for swollen networks.

Acknowledgment. We thank C. Ober for several useful discussions pertaining to the synthesis of PDES chains and T. M. Duncan for his comments on the manuscript. This work was supported by NSF Polymers Program, Grants DMR-9706066 and 0078863. We also made use of the Cornell Center for Materials Research Shared Experimental Facilities, supported through NSF MRSEC Program, Grant DMR-9632275.

References and Notes

(1) Lee, C. L.; Johannson, O. K.; Flanigan, O. L.; Hahn, P. *Polym. Prepr.* **1969**, *10*, 1319.
(2) Beatty, C. L.; Pochan, J. M.; Froix, M. F.; Hinman, D. D. *Macromolecules* **1975**, *8*, 547.
(3) Froix, M. F.; Beatty, C. L.; Pochan, J. M.; Hinman, D. D. *J. Polym. Sci., Polym. Phys. Ed.* **1975**, *13*, 1269.
(4) Beatty, C. L.; Karasz, F. E. *J. Polym. Sci., Polym. Phys. Ed.* **1975**, *13*, 971.
(5) Pochan, J. M.; Beatty, C. L.; Hinman, D. D. *J. Polym. Sci., Polym. Phys. Ed.* **1975**, *13*, 977.
(6) Papkov, V. S.; Godovsky, Yu. K.; Svistunov, V. S.; Litinov, V. M.; Zhdanov, A. A. *J. Polym. Sci., Polym. Phys. Ed.* **1984**, *22*, 3617.
(7) Tsvankin, D. Ya.; Papkov, V. S.; Zhukov, V. P.; Godovsky, Yu. K.; Svistunov, V. S.; Zhdanov, A. A. *J. Polym. Sci., Polym. Phys. Ed.* **1985**, *23*, 1043.
(8) Godovsky, Yu. K.; Papkov, V. S. *Macromol. Chem., Macromol. Symp.* **1986**, *4*, 71.
(9) Pochan, J. M.; Hinman, D. D.; Froix, M. F. *Macromolecules* **1976**, *9*, 611.
(10) Kögler, G.; Loufakis, K.; Möller, M. *Polymer* **1990**, *31*, 1538.
(11) Molenberg, A.; Möller, M. *Macromolecules* **1997**, *30*, 8332.
(12) Zhdanov, A. A. *Polym. Sci. U.S.S.R.* **1989**, *31*, 1729.
(13) Out, G.; Turetskii, A. A.; Snijder, M.; Möller, M.; Papkov, V. S. *Polymer* **1995**, *36*, 3213.
(14) Litvinov, V. M.; Macho, V.; Spiess, H. W. *Acta Polym.* **1997**, *48*, 471.
(15) Godovsky, Yu. K. *Angew. Makromol. Chem.* **1992**, *202/203*, 187.
(16) Papkov, V. S.; Godovskii, Yu. K.; Svistunov, V. S.; Zhdanov, A. A. *Polym. Sci. U.S.S.R.* **1989**, *31*, 1729.
(17) Godovsky, Y. K.; Volegova, I. A.; Valetskaya, L. A.; Rebrov, A. V.; Novitskaya, L. A.; Rotenburg, S. I. *Polym. Sci. U.S.S.R.* **1988**, *30*, 329.
(18) Finlkelmann, H.; Rock, H. J.; Rehage, G. *Makromol. Chem., Rapid Commun.* **1981**, *2*, 317.
(19) Yang, Y.; Kloczkowski, A.; Mark, J. E.; Erman, B.; Bahar, I. *Macromolecules* **1995**, *28*, 4927.
(20) Kirste, R. G.; Ohm, H. G. *Makromol. Chem., Rapid Commun.* **1985**, *6*, 179.
(21) D'allest, J. F.; Sixou, P.; Blumstein, R. B.; Teixeira, J.; Noirez, L. *Mol. Cryst. Liq. Cryst.* **1988**, *155*, 581.
(22) Godovsky, Y. K.; Papkov, V. S. *Adv. Polym. Sci.* **1988**, *88*, 129.
(23) Gilra, N.; Cohen, C.; Panagiotopoulos, A. Z. *J. Chem. Phys.* **2000**, *112*, 6910.
(24) Patel, S. K.; Malone, S.; Cohen, C.; Gillmor, J. R.; Colby, R. H. *Macromolecules* **1992**, *25*, 5241.
(25) Out, G. J. J.; Klok, H. A.; Möller, M.; Oelfin, D. *Macromol. Chem. Phys.* **1995**, *196*, 195.
(26) Hedden, R. C.; Cohen, C. *Polymer* **2000**, *41*, 6975.
(27) Macosko, C. W.; Saam, J. C. *Polym. Bull.* **1987**, *18*, 463.
(28) Takeuchi, H.; Cohen, C. *Macromolecules* **1999**, *32*, 6792.
(29) Saxena, H. M.S. Thesis, Cornell University, Ithaca, NY, 2000.
(30) Stockmayer, W. H.; Fixman, M. *J. Polym. Sci., Part C* **1963**, *1*, 137.
(31) Dondos, A.; Benoit, H. *Polymer* **1978**, *19*, 523.
(32) Miyaki, Y.; Einaga, Y.; Fujita, H.; Fukuda, M. *Macromolecules* **1980**, *13*, 588.
(33) Zimm, B. H. *Macromolecules* **1980**, *13*, 592.
(34) Aven, M. R.; Cohen, C. *Makromol. Chem.* **1988**, *189*, 881.
(35) Fetters, L. J.; Lohse, D. J.; Richter, D.; Witten, T. A.; Zirkel, A. *Macromolecules* **1994**, *27*, 4639.
(36) Fetters, L. J.; Lohse, D. J.; Colby, R. H. In *Physical Properties of Polymers Handbook*; Mark, J. E., Ed.; American Institute of Physics Press: Woodbury, NY, 1996.
(37) Treloar, L. R. G. *The Physics of Rubber Elasticity*; Clarendon Press: Oxford, 1958.
(38) Graessley, W. W. *J. Polym. Sci., Polym. Phys. Ed.* **1980**, *18*, 27.
(39) Shibanov, Yu. D. *Polym. Sci. U.S.S.R.* **1989**, *31*, 2653.
(40) Sivasailam, K.; Cohen, C. *J. Rheol.* **2000**, *44*, 897.
(41) Flory, P. J. *Principles of Polymer Chemistry*; Cornell University Press: Ithaca, NY, 1953.
(42) Flory, P. J.; Rehner, J. *J. Chem. Phys.* **1943**, *11*, 521.
(43) Hedden, R. C.; Wong, C.; Cohen, C. *Macromolecules* **1999**, *32*, 5154.
(44) McKenna, G. B.; Horkay, F. *Polymer* **1994**, *35*, 5737.
(45) McKenna, G. B.; Flynn, K. M.; Chen, Y. *Polymer* **1990**, *31*, 1937.
(46) Horkay, F.; Hecht, A. M.; Geissler, E. *J. Chem. Phys.* **1989**, *4*, 2706.
(47) Obukhov, S.; Rubinstein, M.; Colby, R. H. *Macromolecules* **1994**, *27*, 3191.
(48) Mandelkern, L. *Crystallization of Polymers*; McGraw-Hill: New York, 1956.
(49) Flory, P. J. *J. Am. Chem. Soc.* **1956**, *78*, 5222.
(50) Hedden, R. C.; Tachibana, H.; Cohen, C.; Duncan, T. M. To be submitted to *Macromolecules*.
(51) Godovsky, Y. K.; Valetskaya, L. A. *Polym. Bull.* **1991**, *27*, 221.
(52) De Gennes, P.-G. *C. R. Acad. Sci. Ser.* **1975**, *B281*, 101.
(53) De Gennes, P.-G. In *Polymer Liquid Crystals*; Cifferi, A., Krigbaum, W. R., Meyer, R. B., Eds.; Academic Press: New York, 1982.
(54) Tanaka, T.; Allen, G. *Macromolecules* **1977**, *10*, 426.
(55) Jarry, J. P.; Monnerie, L. *Macromolecules* **1979**, *12*, 316.
(56) Deloche, B.; Samulski, E. T. *Macromolecules* **1981**, *14*, 575.
(57) Warner, M.; Wang, X. J. *Macromolecules* **1991**, *24*, 4932.
(58) Yang, Y.; Kloczkowski, A.; Mark, J. E.; Erman, B.; Bahar, I. *Macromolecules* **1995**, *28*, 4920.
(59) Erman, B.; Bahar, I.; Kloczkowski, A.; Mark, J. E. *Macromolecules* **1990**, *23*, 5335.

MA001419C